SI Appendix

Naked mole rats can undergo developmental, oncogene-induced and DNA damage-induced cellular senescence

Yang Zhao[a,1], Alexander Tyshkovskiy[b,c,1], Daniel Munoz-Espin[d,e], Xiao Tian[a], Manuel Serrano[d,f,g], Joao Pedro de Magalhaes[h], Eviatar Nevo[i,2], Vadim N. Gladyshev[c], Andrei Seluanov[a,2] and Vera Gorbunova[a,2]

[a] Department of Biology, University of Rochester, Rochester, NY 14627, USA;

[b] Center for Data-Intensive Biomedicine and Biotechnology, Skolkovo Institute of Science and Technology, 143028 Moscow, Russia;

[c] Division of Genetics, Department of Medicine, Brigham and Women's Hospital, Harvard Medical School, Boston, MA 02115, USA;

[d] Tumor Suppression Group, Spanish National Cancer Research Centre, Madrid 28029, Spain;

[e] Cancer Research UK Cambridge Centre Early Detection Programme, Department of Oncology, University of Cambridge, Hutchison/MRC Research Centre, Cambridge CB2 0XZ, United Kingdom;

[f] Institute for Research in Biomedicine, Barcelona Institute of Science and Technology, Barcelona 08028, Spain;

[g] Catalan Institute of Advanced Studies, Barcelona 08010, Spain;

[h] Integrative Genomics of Ageing Group, Institute of Ageing and Chronic Disease, University of Liverpool, Liverpool L7 8TX, United Kingdom;

[i] Institute of Evolution, University of Haifa, Haifa 3498838, Israel.

[1] These two authors contributed equally

[2] Corresponding authors

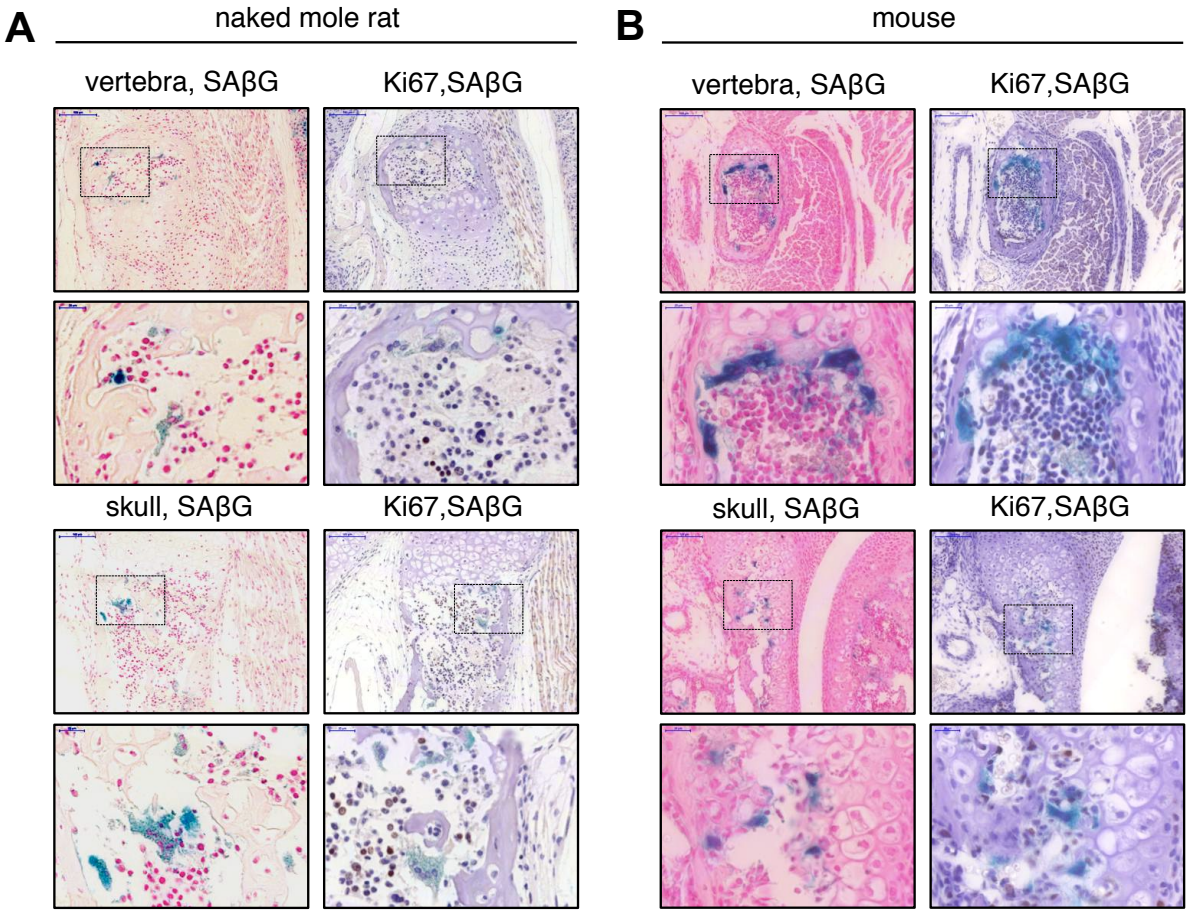

Figure S1. Developmental senescence of naked mole rat (NMR). Senescence-associated β-galactosidase (SA-β-gal) and Ki67 staining in the bone marrow of newborn NMRs (A) and mice (B).

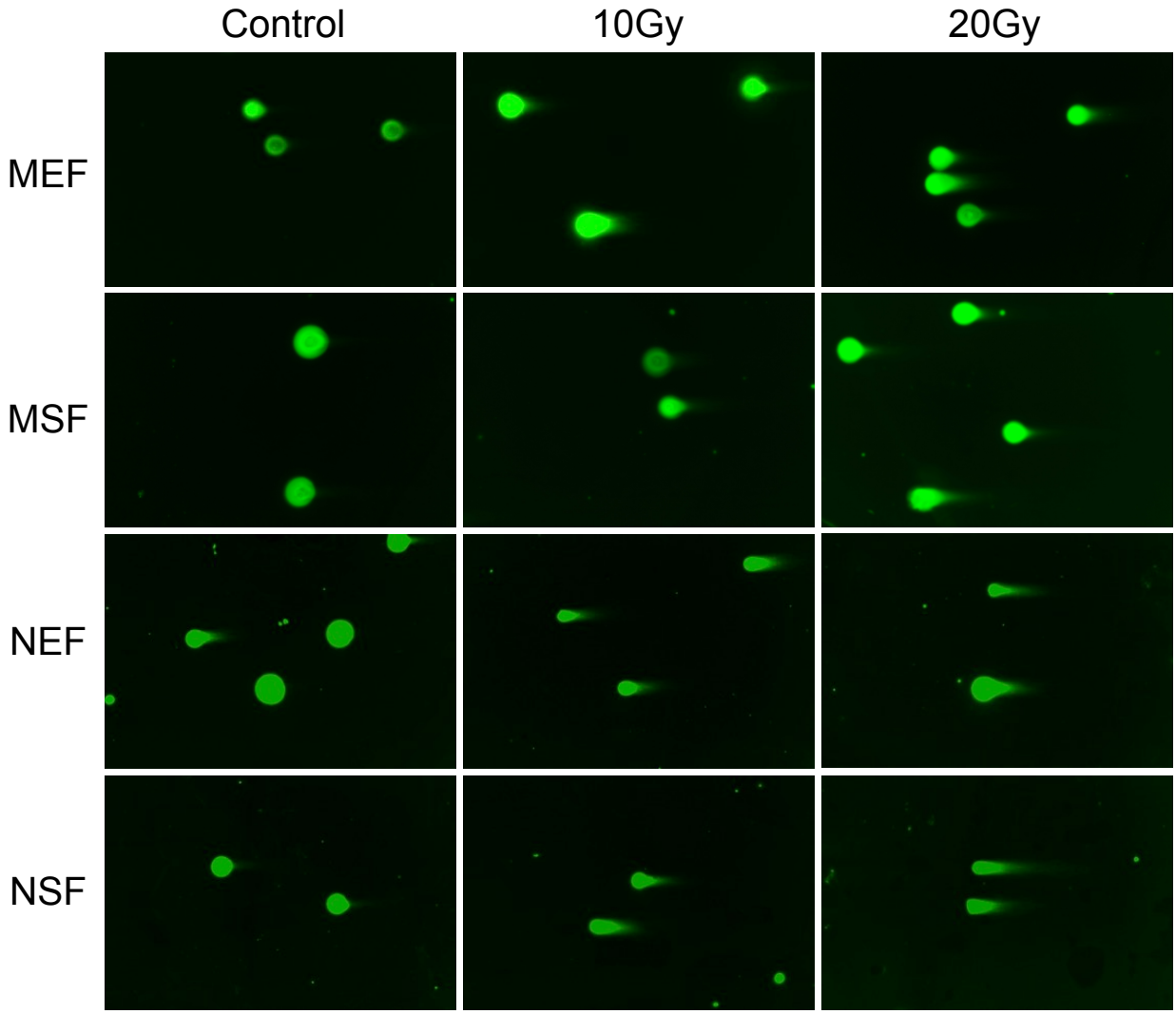

Figure S2. Images of comet assay showing DNA damage in NMR and mouse fibroblasts in response to γ-irradiation. The cells were processed for comet assays immediately after the irradiation.

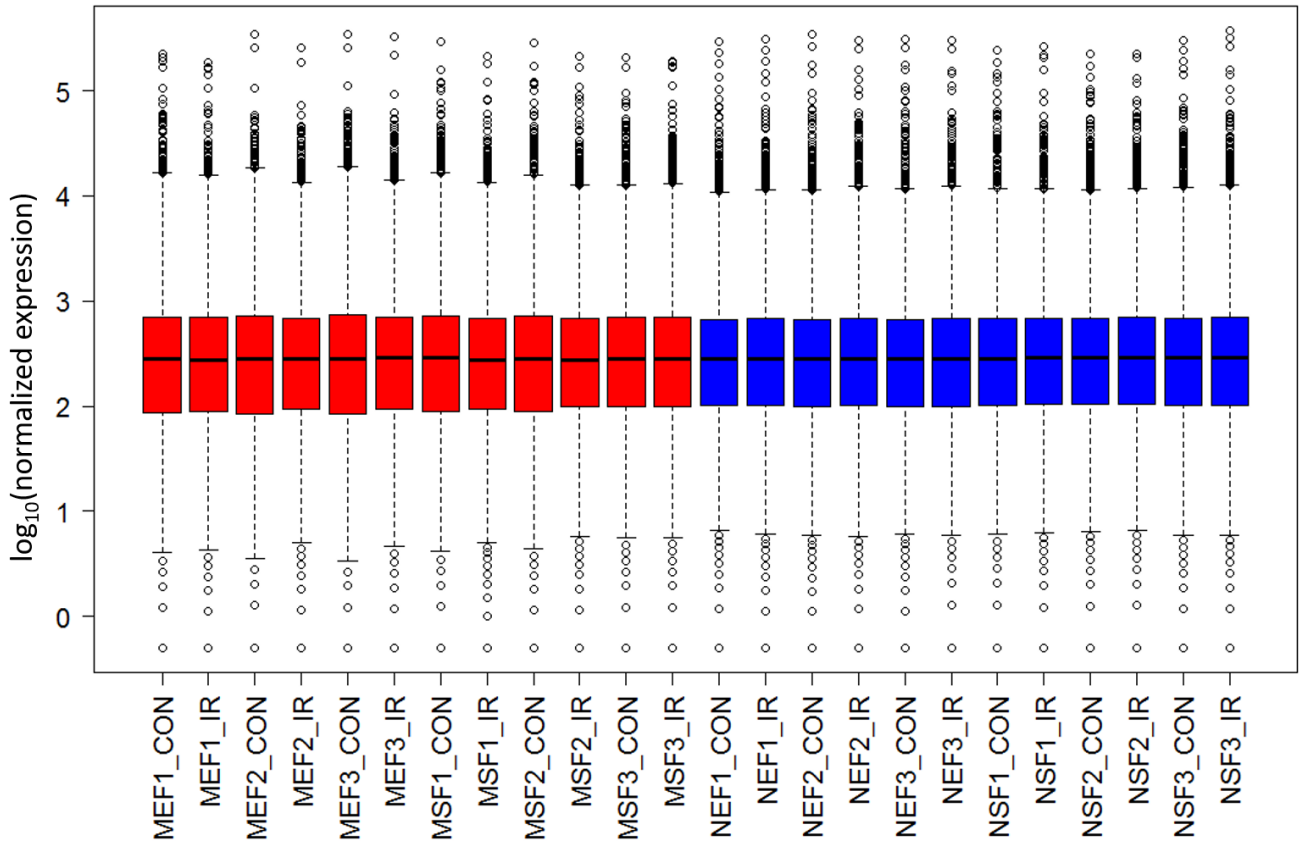

Figure S3. Boxplot of gene expression (in logarithmic scale) of individual samples after filtering out low-expressed genes and RLE normalization. Mouse samples are colored in red and NMR samples in blue. Samples are similarly distributed and don't include technical outliers. NEF: NMR Embryonic Fibroblasts; NSF: NMR Skin Fibroblasts; MEF: Mouse Embryonic Fibroblasts; MSF: Mouse Skin Fibroblasts; CON: Control; IR: γ-irradiation.

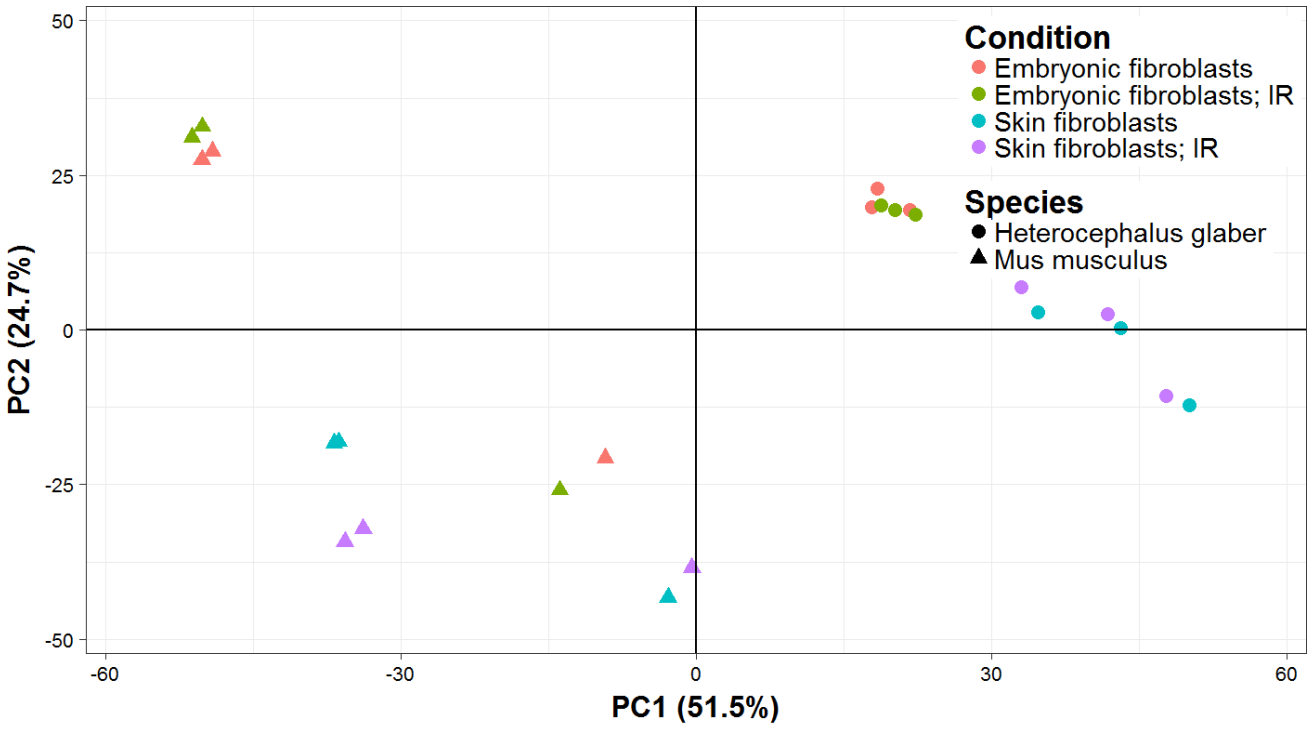

Figure S4. PCA analysis of individual samples. Samples generally cluster by species (first principal component explaining 51.5% of variance). Irradiation samples, as expected, cluster together with their paired controls.

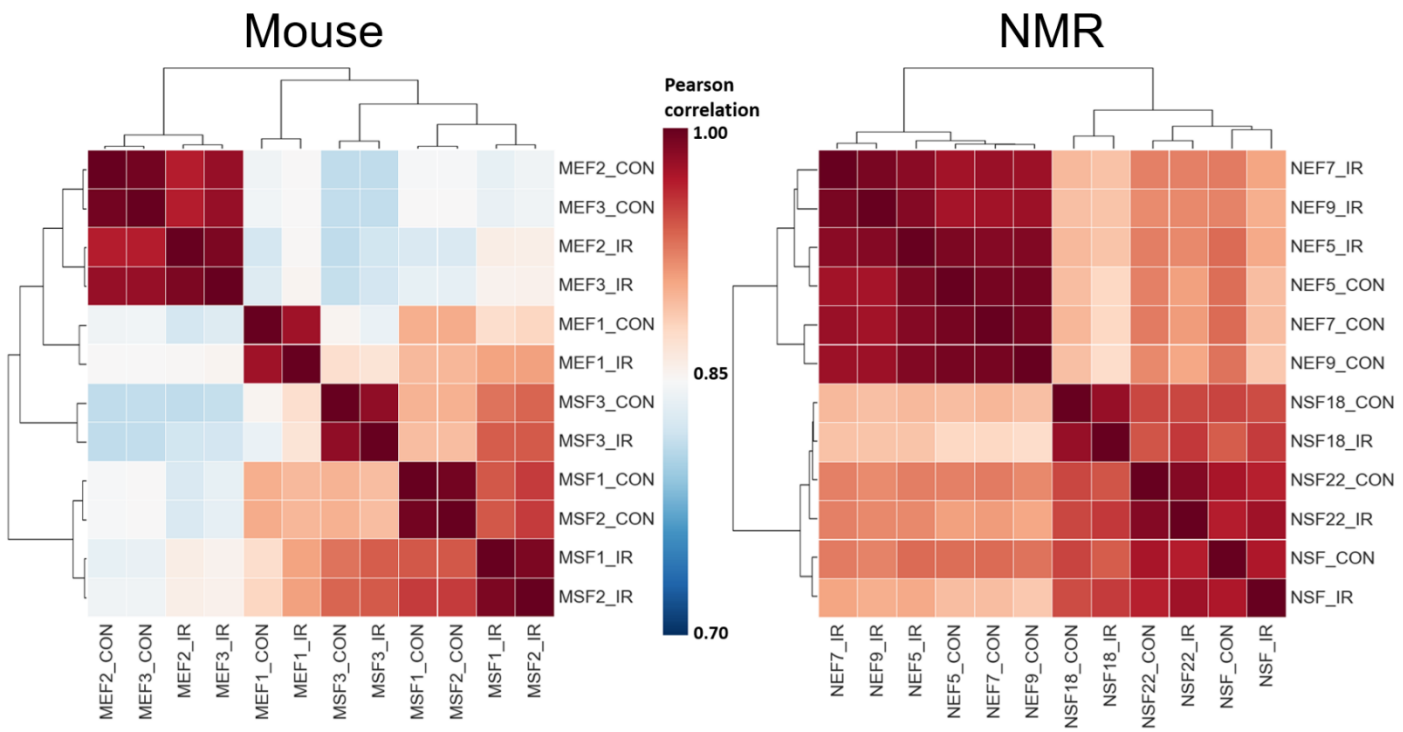

Figure S5. Pearson correlation matrix for mouse (left) and NMR (right) individual samples. Within species, samples generally cluster based on types of fibroblasts. NMR samples show higher similarity across samples compared to mouse samples. NEF: NMR Embryonic Fibroblasts; NSF: NMR Skin Fibroblasts; MEF: Mouse Embryonic Fibroblasts; MSF: Mouse Skin Fibroblasts; CON: Control; IR: After γ-irradiation.

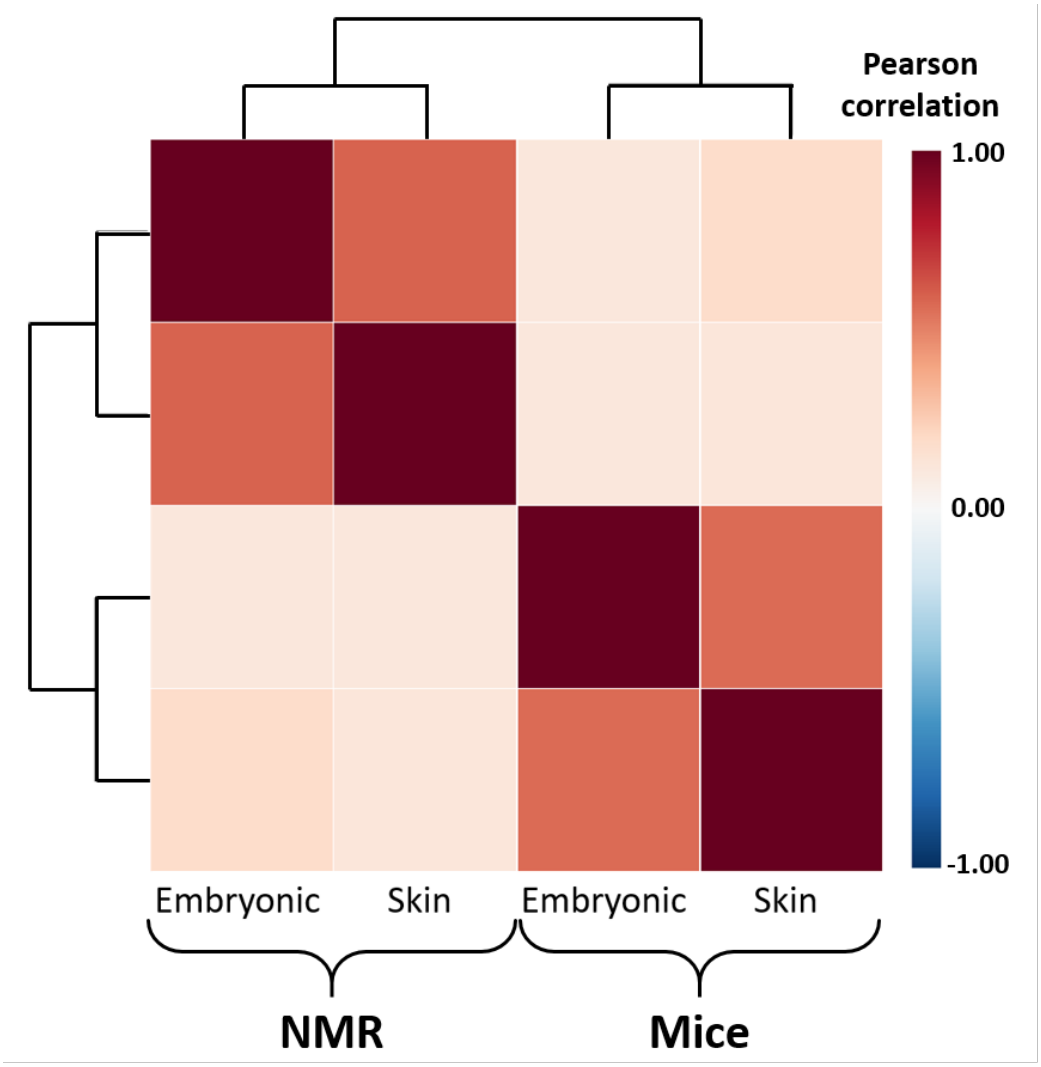

Figure S6. Pearson correlation matrix of aggregated changes induced by IR in NMR and mouse embryonic and skin fibroblasts. Changes are more similar within the same species than within the same cell type. All analyzed groups show significant positive correlation with each other. Embryonic: Embryonic Fibroblasts; Skin: Skin Fibroblasts.

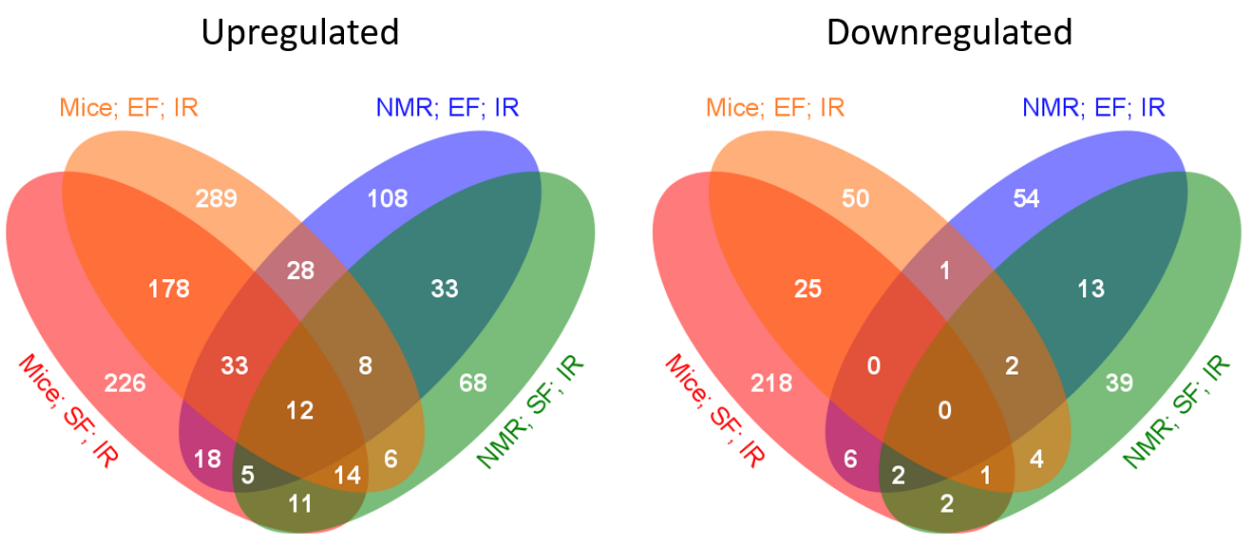

Figure S7. Venn diagram showing numbers of differentially expressed genes (adjusted p-value < 0.05; FC > 2) for each species and type of fibroblasts. Many differentially expressed genes overlap between different analyzed groups, especially between different types of fibroblasts within the same species. EF: Embryonic Fibroblasts; SF: Skin Fibroblasts; IR: After γ-irradiation.

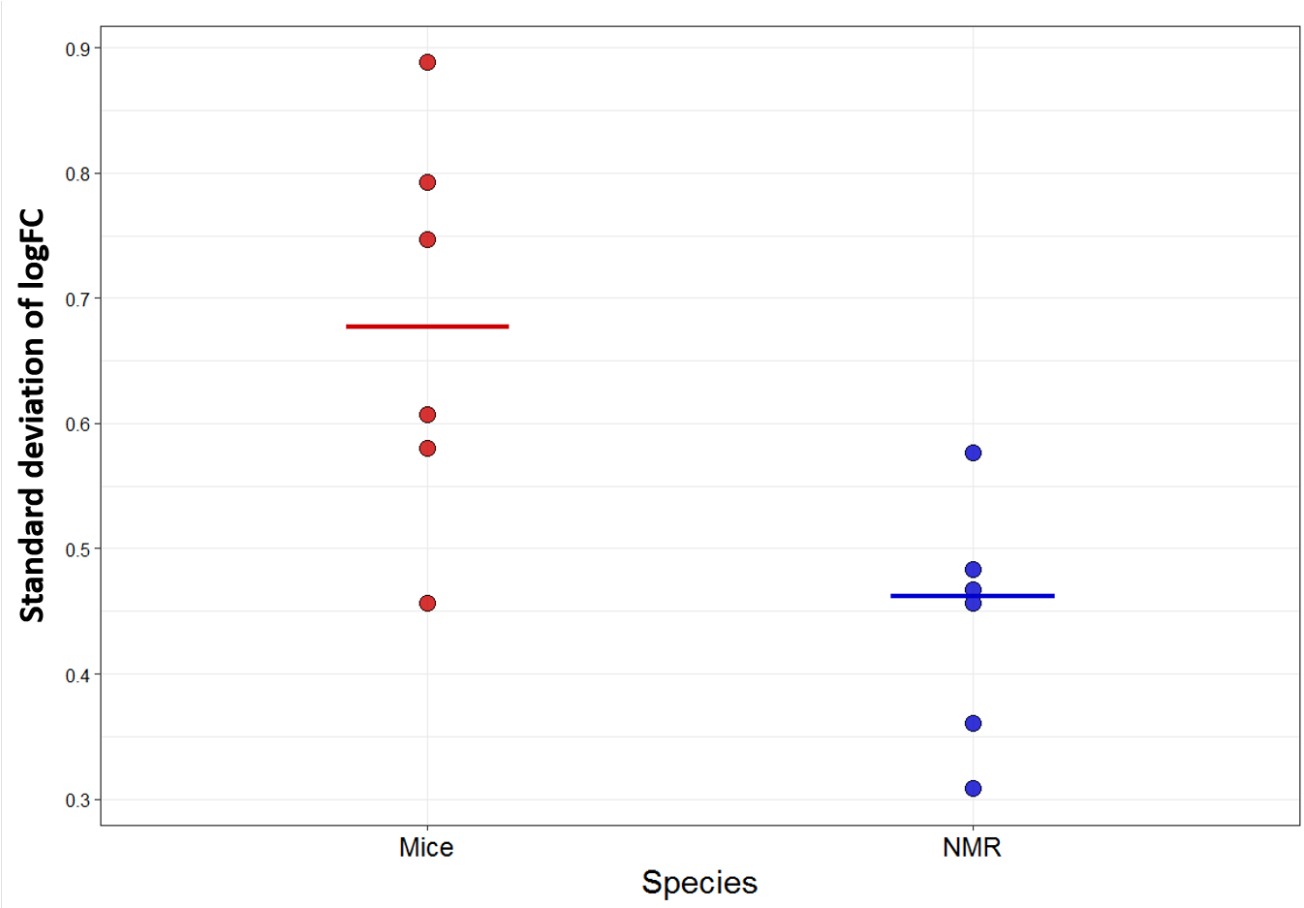

Figure S8. Standard deviations of gene fold changes across mice and NMR samples in response to γ-irradiation. Generally, we observe more drastic changes in mice samples (p-value of unpaired Mann-Whitney test = 0.015), which confirms bigger effect of irradiation on expression of individual genes in mice.

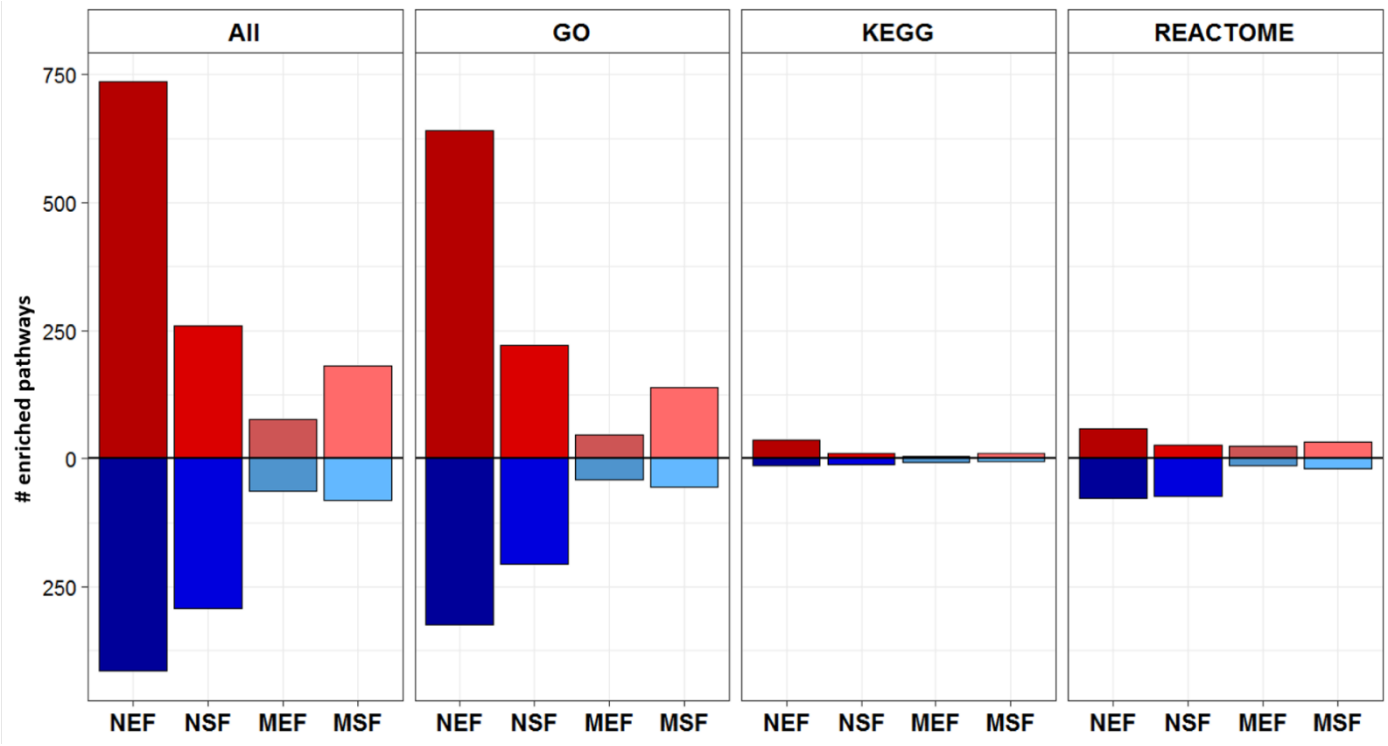

Figure S9. Number of enriched pathways in response to γ-irradiation (q-value < 0.05), according to GSEA, in analyzed groups based on different gene set sources. Red and blue bars show pathways enriched by upregulated and downregulated genes, respectively. Across all gene set sources, number of enriched pathways for both types of fibroblasts in NMR is higher than in mice. NEF: NMR Embryonic Fibroblasts; NSF: NMR Skin Fibroblasts; MEF: Mouse Embryonic Fibroblasts; MSF: Mouse Skin Fibroblasts; GO: Gene Ontology (Biological Process and Molecular Function); KEGG: Kyoto Encyclopedia of Genes and Genomes.

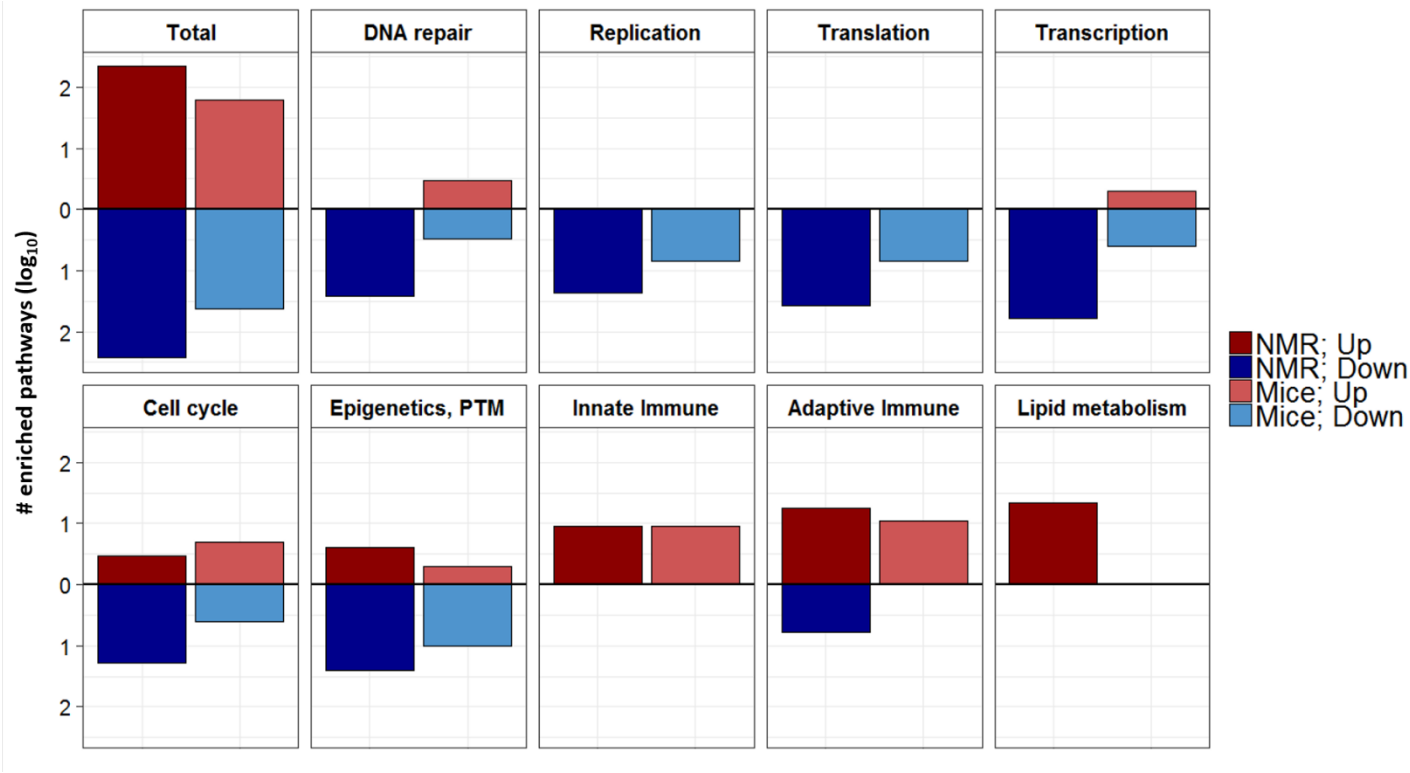

Figure S10. Number of pathways (in logarithmic scale) enriched across both types of fibroblasts in NMR and mice, grouped by belonging to different biological cellular processes, as specified in Supporting Information Dataset 1. NMR fibroblasts show more enriched pathways in response to γ-irradiation compared to mice, although more individual genes are perturbed in mice. Higher number of enriched pathways in NMR across different biological groups can be statistically explained by difference in total number of pathways (z-score proportion test p-value > 0.05). Red and blue bars show pathways enriched by upregulated and downregulated genes, respectively. DNA repair: DNA damage/repair; Replication: DNA replication; Translation: Ribosome/protein translation; PTM: Post-Translational Modification; Innate Immune: Immune response innate; Adaptive Immune: Immune response adaptive/mixed.

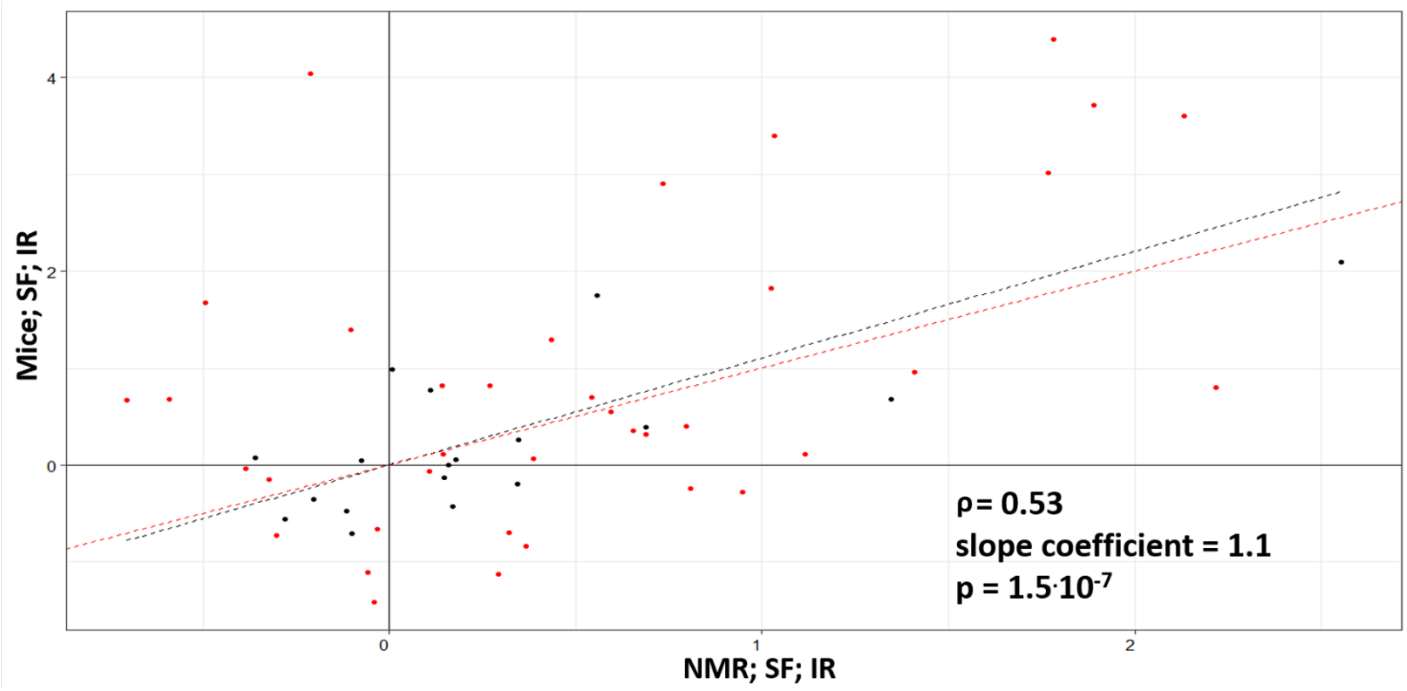

Figure S11. SASP genes show similar behavior among NMR and mouse skin fibroblasts in response to IR (Pearson correlation coefficient = 0.53; p-value = 1.5×10^{-7}) and are changed with similar scale (slope coefficient = 1.1). Genes with significant changes (adjusted p-value < 0.05) in at least one of species are colored in red. Regression and identity lines are shown as black and red dotted line, respectively. SF: Skin Fibroblasts; IR: After γ-irradiation; ρ: Pearson correlation coefficient; p: p-value.

Fig. S12

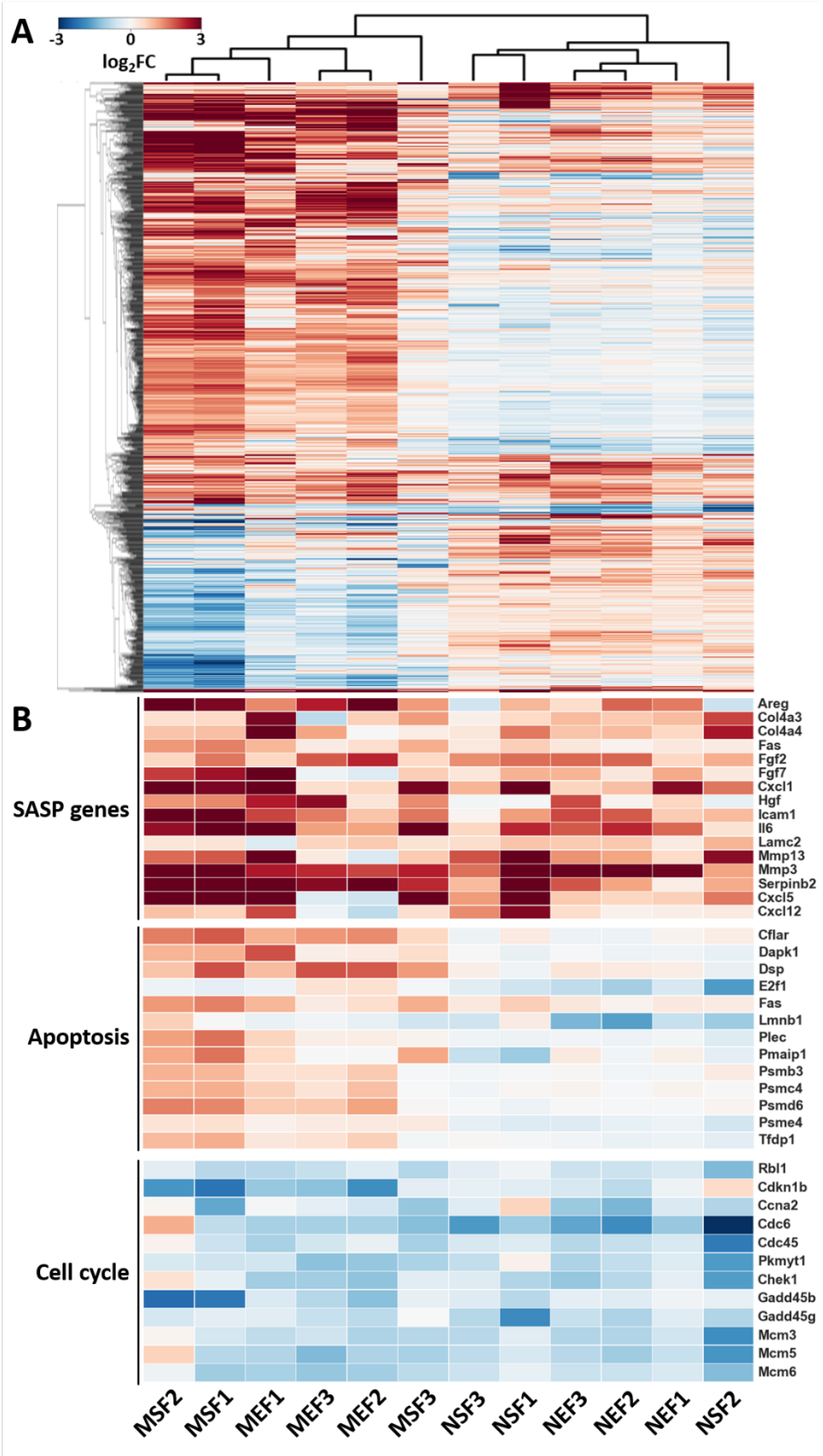
A
-3
0
3
log2FC
B
SASP genes
Areg
Col4a3
Col4a4
Fas
Fgf2
Fgf7
Cxcl1
Hgf
Icam1
Il6
Lamc2
Mmp13
Mmp3
Serpinb2
Cxcl5
Cxcl12
Apoptosis
Cflar
Dapk1
Dsp
E2f1
Fas
Lmnb1
Plec
Pmaip1
Psmb3
Psmc4
Psmd6
Psme4
Tfdp1
Cell cycle
Rbl1
Cdkn1b
Ccna2
Cdc6
Cdc45
Pkmyt1
Chek1
Gadd45b
Gadd45g
Mcm3
Mcm5
Mcm6
MSF2
MSF1
MEF1
MEF3
MEF2
MSF3
NSF3
NSF1
NEF3
NEF2
NEF1
NSF2

Fig. S12B (continued)

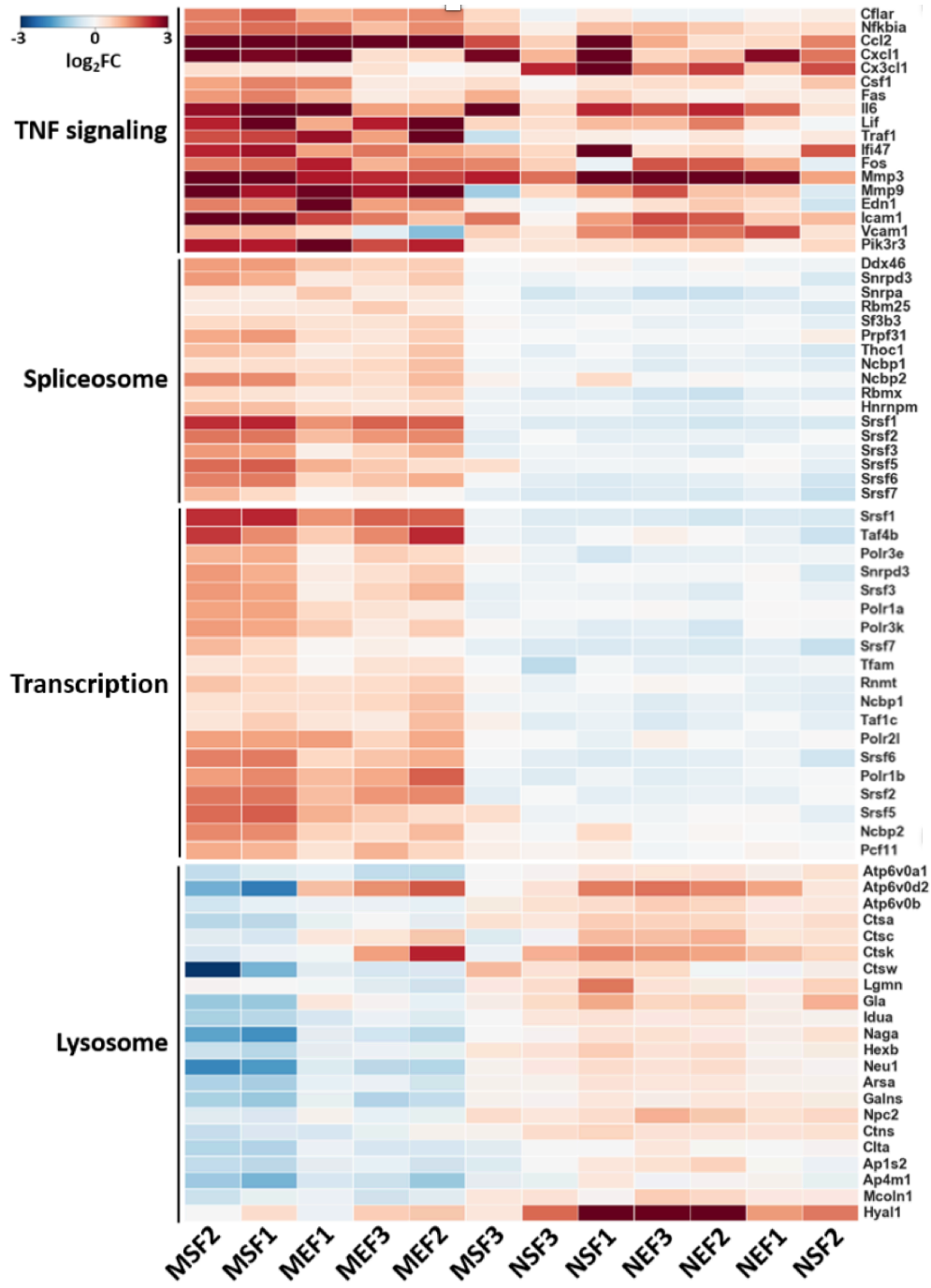

Figure S12. Genes with common and distinct gene expression response to γ-radiation in NMR and mouse fibroblasts. (A) Heatmap of genes identified as commonly or distinctly responded to irradiation in NMR and mouse (Benjamini-Hochberg adjusted p-value < 0.05, fold change > 2 in any direction). 224 genes were identified as commonly changed, and 782 as distinctly changed. (B) Functions enriched by genes with common (SASP genes, Cell cycle, TNF signaling) and distinct (Apoptosis, Transcription, Spliceosome, Lysosome) response to γ-irradiation in NMR and

mouse fibroblasts (q-value < 0.05). Differentially expressed genes (adjusted p-value < 0.05, fold change > 2 in any direction) are shown for each pathway. Commonalities and differences between responses of mouse and NMR observed at the level of functional enrichment are preserved at the level of individual genes. NEF: NMR Embryonic Fibroblasts; NSF: NMR Skin Fibroblasts; MEF: Mouse Embryonic Fibroblasts; MSF: Mouse Skin Fibroblasts; SASP: senescence-associated secretory phenotype.

SI

Materials and Methods

Analysis of Developmental Senescence

SA-β-Gal activity assay. SA-β-Gal staining was performed in whole-mount newborn NMR and mice preserved in OCT using the Senescence β-Galactosidase Staining Kit (Cell Signaling). Briefly, whole tissues were fixed at room temperature, for 45 min, with a solution containing 2% formaldehyde and 0.2% glutaraldehyde in PBS, washed three times with PBS, and incubated overnight at 37 °C with the Staining Solution containing X-gal in N-N-dimethylformamide (pH 6.0). Tissues were subsequently dehydrated with two consecutive steps in 50% and 70% EtOH and embedded in paraffin for serial sectioning. Sections were counterstained with nuclear fast red (NFR) or were processed for immunohistochemistry.

Immunohistochemistry. Newborn NMR and mice were serially sectioned (3 μm thickness) in SuperFrostPlus glass slides (Menzel-Gläser, Braunschweig, Germany) for immunohistochemical studies. In the case of bone marrow sections, tissues were previously decalcified. The slides of interest were then incubated for at least 30 min at 55ºC before being deparaffinized in a clearing agent (xylene) and rehydrated in a descending series of ethanol solutions. Antigen retrieval was carried out in a PTLink instrument (Dako) or in the DiscoveryXT (Ventana). Antibodies against Ki67 (prediluted SP6, Master Diagnostica 0003110QD) were used for both newborn NMR and mice. Immunoreactive cells were visualized using 3,3-diaminobenzidine tetrahydrochloride plus (DAB+) as a chromogen. Sections were counterstained with hematoxylin.

Immunofluorescence. For immunofluorescence, newborn NMR paraffin sections were subjected to antigen retrieval by the use of 0.01 M citrate buffer, pH 6. Then, coverslips were washed three times in PBS, for 10 min each time, permeabilized with 0.1% Triton X-100, for 30 min, and blocked by incubation with 5% fetal calf serum in PBS for 30 min. The coverslips were incubated overnight at 4 °C with antibodies against mouse p21 (HUGO-291, CNIO). After washing three times in PBS with 0.1% Tween 20, for 10 min each time, coverslips were incubated with fluorochrome-conjugated secondary antibodies (linked to Alexa Fluor 555, Life

Technologies). This and all subsequent steps were performed with minimal exposure of samples to light. Coverslips were mounted by using Vectashield Mounting Medium supplemented with 1.5 μg/ml DAPI. The slides were analyzed with a Leica TCS SP5 laser scanning confocal microscope by using the LAS AF v2.6 acquisition software and the HCS-A application.

Cell Culture. Mouse embryonic fibroblasts (MEFs) and skin fibroblasts (MSFs) were grown at 37 °C in an atmosphere of 5% CO_2 and 3% O_2. Naked mole rat (NMR) embryonic fibroblasts (NEFs) and skin fibroblasts (NSFs) were grown at 32 °C (in vivo body temperature of naked mole rat) with 5% CO_2 and 3% O_2. All cells were cultured in EMEM medium (ATCC) with 15% (vol/vol) FBS, 100 μg/mL penicillin, and 100 U/mL streptomycin (Gibco).

Overexpression of Oncogenes. MEF, MSF, NEF, and NSF were transfected with pMaxGFP (Lonza) or pCMV-HRas V12 (Clontech), respectively. Transfection was performed using Amaxa Nucleofector II on program T-020 and solution NHDF (Amaxa). Medium was changed 1 day after transfection, and cells were then maintained for 12 days before senescence-associated β-galactosidase (SA-β-gal) assay.

γ-Irradiation-Induced CS. Growing mouse and naked mole rat fibroblasts were subjected to 10 Gy or 20 Gy γ-irradiation, and allowed to grow for 2 days for BrdU assay and western blot, or 12 days for SA-β-gal assay and RNA extraction for RNA sequencing (RNA-seq).

Western Blotting. Two days after γ-irradiation (IR), cells were harvested and lysed in Laemmli Sample Buffer (Bio-Rad) with 1 mM PMSF. Extracts were boiled and centrifuged at 14,000 × g for 15 min at 4 °C. Protein samples were resolved by SDS-polyacrylamide gel electrophoresis and transferred to PVDF membranes (Bio-Rad). Membranes were incubated with a rabbit monoclonal anti-p21 primary antibody (ab109199; Abcam). A horseradish peroxidase (HRP)-conjugated anti-rabbit IgG (Abcam) secondary antibody was used. Proteins were visualized using an ECL kit (Bio-Rad).

BrdU-Incorporation Assay. Two days after IR, cells were cultured in the presence of BrdU (3 μg/ml) for 48 h, and fixed using 4% paraformaldehyde for 60 min, washed with PBS for 5 times, followed by treatment with 2N HCl for 30 min. After washed with PBS for 3 times, cells were blocked with 5% FBS in PBS with 0.2% Triton X-100 for 2 h. A FITC-conjugated anti-BrdU antibody (Sigma; 1:200) was used to incubate the cells at 4 °C overnight. Cells were then incubated

with Hoechst for 10 min at room temperature, and observed under a fluorescence microscope. Images were acquired for five replicates and counted for at least 100 cells for each replicate.

SA-β-Gal Assay. For SA-β-gal staining, cells were fixed and stained using a commercial senescence β-galactosidase staining kit (Cell Signaling). Images were captured for 5 replicates and counted at least 100 cells for each replicate.

Comet Assay. Cells were kept on ice and subjected to 10 or 20 Gy IR, and were then harvested immediately. DNA damage was detected by using a commercial comet assay kit (Trevigen) following the manufacture. Images were acquired and the percentage of tail DNA was analyzed from 100 cells per sample using CaspLab software.

Flow Cytometry. Mouse and NMR fibroblasts were subjected to 10 or 20 Gy γ-irradiation. Three days after irradiation, cells were harvested and stained using an Annexin V-Fluo staining kit (Roche). Cell death was measured using FACS on a BD LSR II Flow Cytometer.

RNA-seq Data Processing and Analysis. Raw reads generated from the Illumina HiSeq2500 sequencer were demultiplexed using configurebcl2fastq.pl, version 1.8.4. Quality filtering and adapter removal were performed using Trimmomatic version 0.32. Processed/cleaned reads were then mapped with STAR (version 2.5.2b) (1) to the set of orthologs common to naked mole rats and mice (2) to ensure consistent annotation between the species and, therefore, to make them appropriate for subsequent cross-species analyses. Read counting was performed by featureCounts (3). To filter out genes with low number of reads and expressed only in one species, only genes with at least 1 count per million (cpm) in at least 3 samples (25%) in each species were included, which resulted in the expression set of 11,178 genes across 24 samples. Filtered data was then passed through RLE normalization (4).

Principal component analysis (PCA) was performed on the standardized expression values and the first 2 principal components were extracted with the corresponding percentage of explained variance.

Differential expression analysis was performed with the R package edgeR (5). We declared gene expression to be significantly changed, if p-value, adjusted by the Benjamini-Hochberg procedure, was smaller than 0.05 and fold change was larger than 2 in any direction. When identifying commonly changed genes across NMRs and mice, we included factors responsible for each of the 4 phenotype groups (MEF, MSF, NEF and NSF) to the model but specified an IR effect

as a single factor common to all groups, and tested its difference from 0. When identifying genes with the differential response to IR between NMR and mice, we added a factor responsible for the NMR-specific IR effect to the previous model and tested its difference from 0.

Unpaired Mann-Whitney test against two-sided alternative hypothesis was used to examine statistical significance of difference between standard deviations of mice and NMR genes logFC before and after γ-irradiation.

The Z-score proportion test against two-sided alternative hypothesis was used when examining if differences in the number of enriched functions between NMR and mice in each of functional groups (as specified in Supporting Information Dataset 1) could be explained by difference in the number of enriched functions. The total number of enriched functions was considered as the number of trials, and the number of enriched functions corresponding to a particular functional group were considered as the number of successes. The Benjamini-Hochberg method was used to adjust for multiple comparisons. FDR threshold of 0.05 was used to select statistically significant functional groups.

GSEA (6) was performed on a pre-ranked list of genes based on z-scores, calculated as:

$$z\text{-}score = -\ln(pv) \times sgn(lfc),$$

where *pv* and *lfc* are p-value and logFC of certain gene, respectively, based on edgeR output and *sgn* is signum function (is equal to 1 if value is positive, -1 if negative and 0 if equal to 0). REACTOME, KEGG and GO biological process and molecular function from Molecular Signature Database (MSigDB) have been used as gene sets for GSEA (6). q-value cutoff of 0.05 was used to select statistically significant functions.

References cited

1. Dobin A*, et al.* (2013) STAR: ultrafast universal RNA-seq aligner. *Bioinformatics* 29(1):15-21.
2. Ma S*, et al.* (2016) Cell culture-based profiling across mammals reveals DNA repair and metabolism as determinants of species longevity. *eLife* 5.
3. Liao Y, Smyth GK, & Shi W (2014) featureCounts: an efficient general purpose program for assigning sequence reads to genomic features. *Bioinformatics* 30(7):923-930.
4. Anders S & Huber W (2010) Differential expression analysis for sequence count data. *Genome biology* 11(10):R106.
5. Robinson MD, McCarthy DJ, & Smyth GK (2010) edgeR: a Bioconductor package for differential expression analysis of digital gene expression data. *Bioinformatics* 26(1):139-140.
6. Subramanian A*, et al.* (2005) Gene set enrichment analysis: a knowledge-based approach for interpreting genome-wide expression profiles. *Proc Natl Acad Sci U S A* 102(43):15545-15550.